

Joint 3D inversion of nearshore and land MT and CSEM data in coastal areas of volcanic islands: application to the Bouillante geothermal field

S. Védrine^{1,2}, P. Tarits², F. Bretaudeau¹, S. Hautot³, M. Darnet¹

¹BRGM, 3 Av. Claude Guillemin, Orléans 45060, France, s.vedrine@brgm.fr

²Laboratoire GEO-OCEAN UMR6538, UBO, IUEM, Rue Dumont d'Urville, 29280, Plouzané, France, pascal.tarits@univ-brest.fr

¹BRGM, 3 Av. Claude Guillemin, Orléans 45060, France, f.bretaudeau@brgm.fr

³IMAGIR Sarl, 1 rue des Ateliers F, 29290 Saint Renan, France, sophie.hautot@imagir.eu

¹BRGM, 3 Av. Claude Guillemin, Orléans 45060, France, m.darnet@brgm.fr

SUMMARY

A large-scale magnetotelluric (MT) and controlled-source electromagnetic (CSEM) acquisition campaign was conducted around the exploited Bouillante geothermal field in Guadeloupe in the Lesser Antilles, supplemented by a regional airborne transient electromagnetic survey (AEM). The target is the characterization of the geothermal reservoir and the associated clay cap, generally identified by its highly conductive electrical signature, typical of a conventional volcanic geothermal system in an andesite-type geological environment. MT allows targeting the deepest parts of the subsurface, but the natural signal on which it relies is on average weak at low latitudes and can be much weaker than anthropogenic noise, making its use with dense acquisition challenging close to inhabited areas. CSEM allows completing and densifying the data coverage in the most urbanized areas thanks to the use of high power active current sources and less demanding measurement systems. Moreover, MT and CSEM 3D modeling, as well as inversion, in the coastal areas of volcanic islands can be challenging due to numerical errors induced by the presence of the sea/land interface and large variations in nearshore bathymetry and topography. These errors must be estimated and corrected to best invert the field data. Here we present the workflow and results of the 3D CSEM and MT modeling and inversion independently. The resistivity model obtained with CSEM is consistent with the known geology and the 3D MT model, but provides improved resolution as well as new information on the extension of the reservoir nearshore. We also discuss the complementarity between MT and CSEM in this context, and how to perform their joint inversion in order to benefit from the high resolution and sensitivity of CSEM on the first 2 km and the ability of MT to provide deeper information.

Keywords: Joint 3D inversion, Volcanic islands, Geothermal exploration, MT, CSEM

INTRODUCTION

3D exploration with electromagnetic methods in coastal areas of volcanic islands can be challenging due to the high level of anthropogenic noise, proximity to the sea/land interface, strong variations in near-shore bathymetry and topography, and near-surface heterogeneity. To overcome these limitations, our goal is the multi-scale integration of AEM, nearshore and land MT and CSEM to improve the reconstruction of deep geologic structures in 3D by inversion. The contribution of the CSEM method is a key to overcome anthropogenic noise and increase data coverage over urbanized areas while the AEM method aims to constrain the first 200 meters of our model. Finally, MT can reach the deepest part of the subsurface. In order to study how to integrate the different EM data, we apply our methodology to data from a geothermal exploration campaign carried out around the Bouillante geothermal field operated in Guadeloupe, in the

French West Indies.

METHODS

The nearshore and land MT and CSEM acquisition campaign was conducted in the coastal area of Bouillante, near the geothermal power plant. The acquisition setup is shown in Figure 1 with: land CSEM transmitters, nearshore and land CSEM receivers, nearshore and land MT sites and AEM flight lines. In total, during the 2 weeks of acquisition, 5 CSEM transmitters, 70 CSEM receivers and 21 MT sites were deployed in the field. In addition, we obtained permission to use MT data acquired by ORMAT (Owens et al. 2018) for inversion increasing the number of MT sites by 54. This dataset is very dense and diverse and also provides a unique opportunity to develop our multi-method integration of MT, CSEM and AEM.

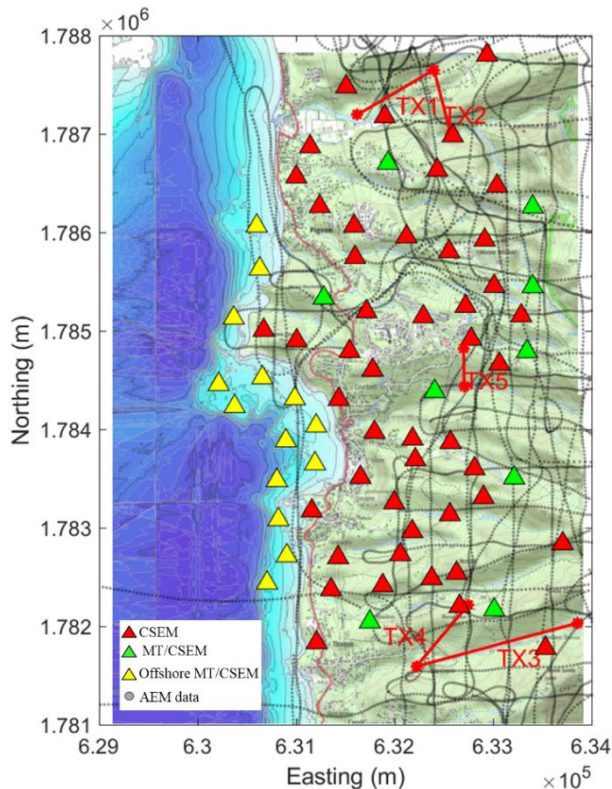


Figure 1. Bouillante survey area. land CSEM transmitters in red lines, land CSEM receivers in red triangles, land MT sites in green and nearshore CSEM receivers and MT sites in yellow. Projected UTM 20 N, WGS 84.

The 3D modeling of CSEM is done with a mixed finite element and finite difference approach using the open-source code *custEM* (Rochlitz et al. 2019), and *POLYEM3D* (Bretaudeau et al. 2021) respectively. The 3D inversion of CSEM data is done with the inversion code *POLYEM3D*, whereas the 3D inversion of MT is done by the code *MINIM3D* (Hautot et al. 2007).

RESULTS

We present a first CSEM 3D inversion result. We used a finite difference modeling grid of about 1.4 million cells. We inverted the real and imaginary part of the electric field in the north and east direction for 5 land transmitters, 70 nearshore and land receivers and for 6 frequencies (between 32 s and 32 Hz). A total of 81,000 parameters were inverted using the Gauss Newton minimization algorithm and using a jacobi-like preconditioner to avoid sensitivity buildup around transmitters and receivers and ensure convergence to a smooth solution. The starting model was an isotropic homogeneous medium of 20 $\Omega\cdot\text{m}$ incorporating nearshore bathymetry variations with seawater fixed at 0.25 $\Omega\cdot\text{m}$ and topography variations. Figure 2 shows the inverted model after

12 GN iterations among with bathymetry and the topographic relief map, the "Plateau" fault (Calcagno et al. 2012), and two geothermal wells.

This first result is in good agreement with both the previous MT 3D inversion from ORMAT and our new 3D MT model. A clay cap is inferred on the shallow part of the model. A low resistive zone is inferred along the "Plateau" fault crossed by a production well. A resistive structure is inferred not far north of the production well, and remains to be interpreted. Finally, from -2000 m below sea level, a low resistive zone is inferred that could be related to the temperature increase, but a sensitivity study remains to be done to confirm its existence. Although this result is interesting, it should be improved by combining it with the new MT 3D inversion which includes new nearshore marine sites and with the AEM logs.

DISCUSSION

The methodology for joint inversion of MT and CSEM data can be based on several strategies, such as cooperative, successive or joint inversion. Choosing one or the other inverted model as a prior or starting model to constrain the inversion of the other method is key to improving the physical and geological consistency of our final inverted resistivity model. A pitfall could be to perform a joint inversion from a blank starting model without further thought, and face minimization problems because MT and CSEM, although based on the same physics and inverting the same parameter, have different resolutions and sensitivities to subsurface anomalies. In the coastal areas of volcanic islands, one may choose to first constrain the deep geological structures by performing a MT inversion, and then add another layer of refinement by inverting the CSEM data. On the other hand, the MT inversion may benefit from the AEM and CSEM data to constrain the near surface and intermediate depth. Ultimately we plan to perform a joint inversion of the MT and CSEM data with the prior constraint of the AEM data, and adapt the relative weight of either method during the inversion process.

CONCLUSIONS

We have shown that CSEM can lead to results in good agreement with previous investigations of the area, and furthermore highlight new features that still need to be rigorously interpreted geologically. This dataset is a unique opportunity to develop a multi-method integration and define the best joint inversion methodology between MT, CSEM and AEM. We will likely begin by performing successive inversion tests to evaluate the best case scenario of

whether MT or CSEM should be inverted first. Then, we will try to adapt our inversion code to perform joint inversion with adaptive weights between both methods.

ACKNOWLEDGEMENTS

This work was conducted under the TEC project funded by the European program Interreg Caribbean. We thank our partners ADEME, OECS, Region Guadeloupe, MAPPEM Geophysics and the computing center occigen of CINES. We particularly thank ORMAT for allowing us to use their MT data.

REFERENCES

- Bretaudeau F., Dubois F., Bissavetsy Kassa S. G., Coppo N., Wawrzyniak P., & Darnet M. (2021). Time-lapse resistivity imaging: CSEM-data 3-D double-difference inversion and application to the Reykjanes geothermal field. *Geophysical Journal International*, 226(3), 1764-1782.
- Calcagno P., Bouchot V., Thinon I., & Bourguine B. (2012). A new 3D fault model of the Bouillante geothermal province combining land and offshore structural knowledge (French West Indies). *Tectonophysics*, 526, 185-195.
- Hautot S., Single R.T., Watson J., Harrop N., Jerram D.A., Tarits P., Whaler K., & Dawe D. (2007). 3-D magnetotelluric inversion and model validation with gravity data for the investigation of flood basalts and associated volcanic rifted margins. *Geophysical Journal International*, 170(3), 1418-1430.
- Owens L., Perkin D., & Garanzini S. (2018). 3D MT Characterization of the Bouillante Geothermal Resource.
- Rochlitz R., Skibbe N., & Günther T. (2019). custEM: Customizable finite-element simulation of complex controlled-source electromagnetic data. *Geophysics*, 84(2), F17-F33.

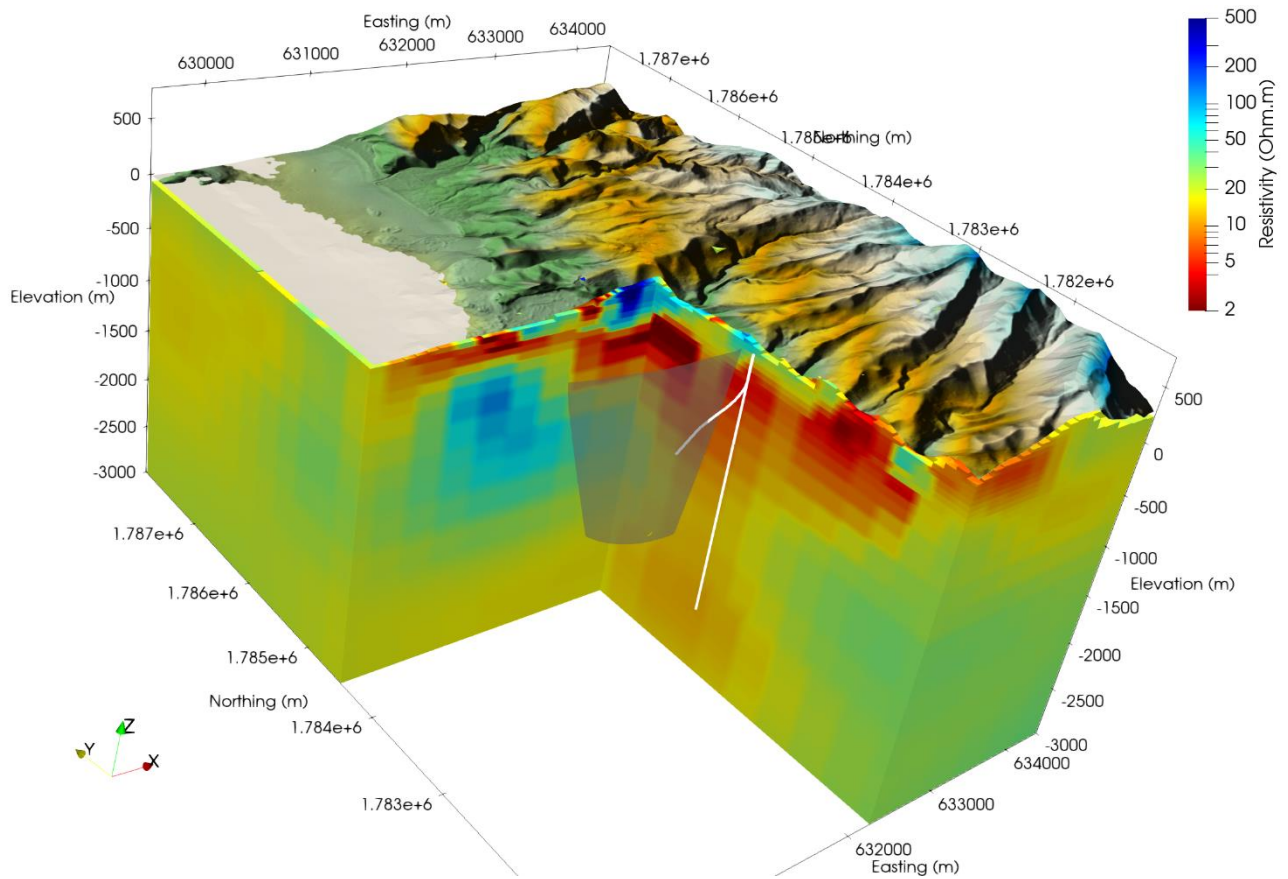


Figure 2. 3D CSEM inversion result after 12 GN iterations, warm colors correspond to low resistivity areas and cold colors to more resistive areas. Variations in bathymetry and topography are shown on top of the model. Two wells of the Bouillante geothermal plant are shown in white. The "Plateau" fault is shown in gray transparency (Calcagno et al. 2012). Projected UTM 20 N, WGS 84.